Sub-Block Level Interference Exploitation Precoding in Satellite Communications

Zhongxiang Wei, *Member, IEEE,* Jingjing Wang, *Member, IEEE,* Christos Masouros, *Fellow, IEEE,* Tongyang Xu, *Member, IEEE,* Jianrui Chen, *Student Member, IEEE,* Ang Li, *Member, IEEE*

***Abstract*—While symbol-level (SL) precoders have been shown to improve transmission performance by treating multi-user interference (MUI) as a useful resource, the SL precoders only employ uniform modulation for all downlink users, and the incurred complexity increases linearly with the block length. In this letter, we investigate the possibility of mixed-modulations interference exploitation (IE) for satellite communications, at a sub-block level. By exploiting the specific detection regions of constellation points of different modulations, a novel sub-block level mixed-modulation (BL-MIE) design is proposed, guaranteeing that MUI is always constructive in each sub-block duration, regardless of the users' heterogeneous modulation schemes. Compared to the classic SL design, it is proved that the BL-MIE provides complexity reduction on the order of square root of the sub-block length, i.e., $\mathcal{O}(\sqrt{n})$, with n denoting the number of symbols per sub-block. Hence, it well strikes the balance between the performance and complexity. Simulation demonstrates that the proposed designs significantly outperform the benchmarks in terms of power consumption and throughput performance.**

***Index Terms*—Interference exploitation, Satellite Communications, Mixed-modulation , Multi-antenna users, Sub-block design, Heterogeneous throughput**

I. Introduction

Towards offering broadband services and planned integration with 5G, the reinvention of satellite communication systems has motivated academia and industry sectors to seek new avenues to augment capacity. Due to the scarcity in frequency bands, a promising approach is to reuse the existing spectrum bands through advanced interference management techniques. Interference exploitation (IE) precoding, which is able to improve the power efficiency of downlink transmission, has recently attracted much attention in both academia and industry. It builds in the principle that multiuser interference (MUI) is not necessarily to be cancelled as a harmful element, which instead can be aligned constructively to the signal of interest at each user. Since the MUI acts as a helpful element, it is able to push the received signal away from the decision thresholds of the constellation, thus significantly improving receiver performance compared to the interference mitigation (IM) based precoders [1] [2]. IE was firstly introduced in code division multiple access systems [3], and then is extended into multi-antenna communications, where [1] demonstrated that the downlink MUI can be constructive by symbol-level (SL) correlation rotation. Recently, the concept of IE has been applied into multiple-input and single-output (MISO) transmission [4], massive antenna-array [5], digital and analogue hybrid beamforming [6], multi-cell coordinated precoding [7], directional modulation [8], and physical layer security [9].

Nevertheless, a number of research challenges remain open in the IE design. 1) The existing IE designs belong to the family of SL precoding. Though our recent prototype in [11] proved the practicality of the SL design, such a symbol-by-symbol optimized design still incurs a high level of complexity. For a block consisting of N symbols, the existing SL precoders need to be solved N times for each block [12]. When the users are equipped with multiple antennas, a typical multiuser multiple-input and multiple-output (MU MIMO) scenario, how to accordingly design a mixed-modulation IE precoder with affordable complexity has yet to be explored. 2) In practice, downlink users have heterogeneous throughput requirements, and are served with distinct modulation schemes in a power-efficient manner. It is because employing high order modulation for the users having low throughput may lead to unnecessary transmission power consumption as well as a high level of bit error rate. On the other hand, employing low order modulation may not satisfy the users' high throughput requirement. Although the concept of IE has been investigated for the uniform modulation scheme, i.e., all the users employing phase shift keying (PSK) [7] [8] or quadrature amplitude modulation (QAM) [10], its feasibility with mixed-modulation is still unknown. More importantly, how to guarantee the constructive effect of the composite MUI for all the users in each sub-block duration, is an open issue.

To address the open issues, we give a first attempt to investigate sub-block level mixed-modulation based IE precoding for MU MIMO systems. Our contributions can be summarized as:

- To the best of our knowledge, it is the first work explicitly investigating the feasibility of sub-block level mixed-modulation for IE design. Focusing on a MU MIMO scenario, a unified framework of mixed modulation IE is formulated. By carefully exploiting the specific available constructive regions of PSK and multi-level modulations, the composite MUI can be made always constructive for

Zhongxiang Wei is with the College of Electronic and Information Engineering, at Tongji University, Shanghai, China. Email: z_wei@tongji.edu.cn

Jingjing Wang and Jianrui Chen are with the School of Cyber Science and Technology, Beihang University, Beijing, China. Email: {drwangjj, chen_jr}@buaa.edu.cn

Christos Masouros is with with the department of Electronic and Electrical Engineering, University College London, London, UK. Email: c.masouros@ucl.ac.uk

Tongyang Xu is is with with the department of Electronic and Electrical Engineering, Newcastle University, Newcastle, UK. Email: tongyang.xu@newcastle.ac.uk

Ang Li is with the School of Information and Communications Engineering, Xi'an Jiaotong University, Xi'an, China. Email: ang.li.2020@xjtu.edu.cn

all users in each sub-block duration.

- A sub-block mixed-modulation IE (BL-MIE) based joint combiner and precoder design is proposed to minimize transmission power, under the users' heterogeneous throughput requirements. In particular, the proposed BL-MIE design leverages the largest singular value of the users' MIMO channel for the users' combiner design, while its precoder guarantees the beneficial effect of the MUI regardless of the PSK or multi-level modulation users. More importantly, compared to the classic SL precoder, the BL-MIE precoder is only optimized across n consecutive symbol-slots, and suppresses the complexity on the order of $\mathcal{O}(\sqrt{n})$, with n denoting the length of each sub-block.

Notations: Matrices and vectors are represented by boldface capital and lower case letters, respectively. $|\cdot|$ denotes the absolute value. $||\cdot||$ denotes the Euclidean-norm operation.

II. System Model

We consider a downlink MU MIMO system, where the base station (BS) equipped with N_t antennas communicates with K users, while each user is equipped with N_r antennas. Assume that there are K_1 ($K_1 = |\mathbb{K}_1|$) users having low/moderate throughput requirement supported by low-order PSK modulation, and K_2 ($K_2 = |\mathbb{K}_2|$) users requiring high throughput with high-order multi-level modulation ($K_1 + K_2 = K$). To avoid confusion, denote i as the i-th PSK modulation user, while denote j as the j-th user supported by multi-level modulation. We consider a spatial-diversity based MIMO, where the BS sends one data stream to each user, and the multi-dimension received signal is equalized at each user with a local combiner to enhance the receive diversity. The BS has knowledge of all users' data and downlink channel state information (CSI), while each user only has knowledge of their own CSI.

Define N as the block-length. Each block can be divided into N/n uniform sub-blocks, i.e., each sub-block consisting n symbols. Define $\boldsymbol{s}^{(\iota)} \in \mathbb{C}^{K\times 1}$ as the symbol vector for the K users in the ι-th symbol slot. Denote $\boldsymbol{W} \in \mathbb{C}^{N_t\times K}$ as the sub-block level precoder at the BS. In the ι-th symbol slot, the received signal at the i-th PSK modulation user is given as

$$\boldsymbol{y}_i^{(\iota)} = \boldsymbol{H}_i\boldsymbol{W}\boldsymbol{s}^{(\iota)} + \boldsymbol{z}_i, \forall i \in \mathbb{K}_1, \tag{1}$$

where $\boldsymbol{H}_i \in \mathbb{C}^{N_r\times N_t}$ represents flat-fading channel from the BS to the i-th PSK user. For a block-level fading channel [1] [6], the superscript symbol slot index is omitted. $\boldsymbol{z}_i \in \mathbb{C}^{N_r\times 1}$ is the circularly symmetric complex Gaussian noise, i.e., $\boldsymbol{z}_i \sim \mathbb{CN}(\boldsymbol{0}, \sigma^2\boldsymbol{I}_{N_r})$. With a local combiner $\boldsymbol{c}_i \in \mathbb{C}^{1\times N_r}$, the post-combined signal is given as

$$r_i^{(\iota)} = \boldsymbol{c}_i\boldsymbol{H}_i\boldsymbol{W}\boldsymbol{s}^{(\iota)} + \boldsymbol{c}_i\boldsymbol{z}_i, \forall i \in \mathbb{K}_1, \tag{2}$$

which is finally used for demodulation and decoding purpose. The above analysis is readily applicable to the multi-level modulation users, which is omitted to avoid repetition.

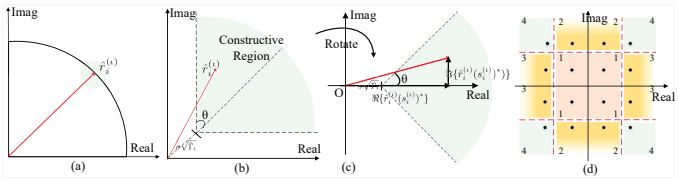

Fig. 1. (a) Conventional IM precoder makes the intended signal locate in a proximity region around the constellation point. (b) PSK based IE precoder pushes the symbol desired signal away from the decision thresholds, i.e, the real and imaginary axes of the quadrature phase shift keying (QPSK) modulation. (c) After rotation by $\angle(s_i^{(\iota)})^*$, the trigonometry can be exploited as shown by (3). (d) For multi-level modulation users, their constructive regions depend on the specific detection regions of the constellation points.

III. Sub-Block Level Mixed Modulation based IE

Classical IM approaches aim to suppress interference such that each user's signal is contained within a region around the nominal point in the modulated signal constellation, as illustrated in Fig. 1(a). In practice, since the transmitted symbol vector $\boldsymbol{s}^{(\iota)}$ is naturally known at the BS, it is possible to jointly utilize the spatial correlation between the users' channel and the data symbols for MUI exploitation. In particular, MUI becomes constructive if it pushes the received signal away from the detection threshold of the signal modulation constellation. This gives rise to the constructive regions, represented by the green areas in Figs. 1(b) and (d) [7]. In the following, we briefly introduce the fundamentals of IE under PSK and multi-level modulation.

IE Precoder for PSK Modulation: In Fig. 1(b), write $\hat{r}_i^{(\iota)} = \boldsymbol{c}_i\boldsymbol{H}_i\boldsymbol{W}\boldsymbol{s}^{(\iota)}$ as the noise-excluding received signal, and $s_i^{(\iota)}$ as the i-user's desired symbol in the ι-th symbol slot. For guaranteeing IE with generic Q-size PSK constellation, the rotated signal $\hat{r}_i(s_i^{(\iota)})^*$ in Fig. 1(c) should satisfy the following inequality as

$$\begin{aligned}|\Im\{\hat{r}_i^{(\iota)}(s_i^{(\iota)})^*\}| \leq \\ (\Re\{\hat{r}_i^{(\iota)}(s_i^{(\iota)})^*\} - \sigma\sqrt{\bar{\Gamma}_i})\tan\theta, \forall i \in \mathbb{K}_1, \forall \iota\end{aligned} \tag{3}$$

where $\Re$ and $\Im$ denote the real and imaginary parts of a complex value, respectively. $\theta = \pi/Q$. $\bar{\Gamma}_i$ denotes the i-th user's subscribed SINR threshold that matches their modulation size and throughput requirement.

IE Precoder for Multi-Level Modulation: With multi-level modulation, the constructive regions depends on the specific detection regions of constellation points. Without loss of generality, 16-quadrature amplitude modulation (QAM) is considered, as illustrated by Fig. 1(d). For the group of constellation points in the box labelled "1": since the constellation points are located in the inner layer of the constellation, they are surrounded by the decision boundaries. As a result, there is no constructive regions for IE, and one should guarantee that the received signal approaches the exact constellation point so as not to exceed the decision boundaries. Hence, for any j-th user in $\mathbb{K}_2$, the IE constraint is

$$\Re\{\hat{r}_j^{(\iota)}\} = \sigma\sqrt{\bar{\Gamma}_j}\Re\{s_j^{(\iota)}\}, \text{ and } \Im\{\hat{r}_j^{(\iota)}\} = \sigma\sqrt{\bar{\Gamma}_j}\Im\{s_j^{(\iota)}\}. \tag{4}$$

For the group of constellation points labelled "2": since the real axis are surrounded by the decision boundaries, the

constructive regions (green area) are infinitely extended along the imaginary axis. Hence, the IE precoder should push the received signals away from the imaginary axis, written as

$$\Re\{\hat{r}_j^{(\iota)}\} = \sigma\sqrt{\bar{\Gamma}_j}\Re\{s_j^{(\iota)}\},\ \text{and}\ \Im\{\hat{r}_j^{(\iota)}\} \geq (\text{or}\ \leq)\sigma\sqrt{\bar{\Gamma}_j}\Im\{s_j^{(\iota)}\}. \tag{5}$$

For the group of constellation points labelled "3": The IE precoder pushes the signals away from the decision boundaries, i.e., the real axis. Hence, the constraints are

$$\Im\{\hat{r}_j^{(\iota)}\} = \sigma\sqrt{\bar{\Gamma}_j}\Im\{s_j^{(\iota)}\}\ \text{and}\ \Re\{\hat{r}_j^{(\iota)}\} \geq (\text{or}\ \leq)\sigma\sqrt{\bar{\Gamma}_j}\Re\{s_j^{(\iota)}\}, \tag{6}$$

For the group of constellation points labelled "4": since the constellation points are not surrounded by the decision boundaries, the constructive regions can be extended infinitely. Hence, the IE constraints are written as

$$\begin{aligned} &\Re\{\hat{r}_j^{(\iota)}\} \geq (\text{or}\ \leq)\sigma\sqrt{\bar{\Gamma}_j}\Re\{s_j^{(\iota)}\}, \text{and} \\ &\Im\{\hat{r}_j^{(\iota)}\} \geq (\text{or}\ \leq)\sigma\sqrt{\bar{\Gamma}_j}\Im\{s_j^{(\iota)}\}. \end{aligned} \tag{7}$$

Based on the above formulations, we target at minimizing power consumption subject to users' subscribed SINR requirements, by jointly designing sub-block level precoder at the BS and the combiner at the users.

$$\begin{aligned} P1\ :\ &\underset{\boldsymbol{W},\boldsymbol{c}_i,\boldsymbol{c}_j}{\text{argmin}}\ \textstyle\sum_{\iota=1}^{n}||\boldsymbol{W}\boldsymbol{s}^{(\iota)}||^2, \\ \text{s.t.}\ &(C1): \hat{r}_i^{(\iota)} = \boldsymbol{c}_i\boldsymbol{H}_i\boldsymbol{W}\boldsymbol{s}^{(\iota)}, \forall i \in \mathbb{K}_1, \forall \iota \in n, \\ &(C2): \hat{r}_j^{(\iota)} = \boldsymbol{c}_j\boldsymbol{H}_j\boldsymbol{W}\boldsymbol{s}^{(\iota)}, \forall j \in \mathbb{K}_2, \forall \iota \in n, \\ &(C3): (3), \forall i \in \mathbb{K}_1, \forall \iota \in n,\ (C4): (4)-(7), \forall j \in \mathbb{K}_2, \forall \iota \in n, \end{aligned} \tag{8}$$

where (C1) and (C2) define the noise-excluding post-combined signal $\hat{r}_{i(\text{or } j)}$ with the effect of the local combiner $\boldsymbol{c}_{i(\text{or } j)}$. (C3) represents the IE conditions of the PSK modulation users, and (C4) represents the IE conditions of the multi-level modulation users. In particular, the embedded SINR requirements in the constraints (C3) and (C4) can be accordingly pre-set based on the specific throughput requirement and the adopted modulation size.

IV. Mixed-Modulation IE based Joint Combiner and Precoder Design

As mentioned in section III, the IE precoder utilizes the knowledge of both channel and data symbols to exploit interference, while each user has knowledge of only their own downlink channel. Due to the asymmetry of design information at the BS and users, the design of the precoder and combiner in P1 has to be decoupled. Hence, we first design the channel-only depended combiner at the users. Since the combiner aims to maximize receive diversity, it is known that the optimal design is based on the singular-value-decomposition (SVD) of $\boldsymbol{H}_i$ as

$$\boldsymbol{H}_i = \boldsymbol{U}_i\boldsymbol{\Lambda}_i\boldsymbol{V}_i^H, \forall i \in \mathbb{K}_1, \tag{9}$$

where $\boldsymbol{U}_i$ and $\boldsymbol{V}_i$ are unitary-matrices. WE write $\boldsymbol{U}_i$ as

$$\boldsymbol{U}_i = [\boldsymbol{u}_1, ..., \boldsymbol{u}_{N_r}], \tag{10}$$

where $\boldsymbol{u}_p \in \mathbb{C}^{N_r \times 1}$ denote the p-th column of the matrix $\boldsymbol{U}_i$. Hence, at the i-th PSK user, it uses the Hermitian transpose of first column of $\boldsymbol{U}_i$ as its combiner, i.e., $\boldsymbol{c}_i = \boldsymbol{u}_1^H$. Physically, it corresponds the largest singular value of the channel $\boldsymbol{H}_i$ and thus demonstrates the highest channel gain. Since the above design can be straightforwardly applied for multi-level modulation, the combiner design for the multi-level modulation user is omitted to avoid repetition.

Now, we turn to handle the precoder design, where the difficulty lies in how to give a unified IE constraint for the users with distinct modulation schemes. Since the IE condition of the multi-level modulation users depends on the specific modulation points, we define a set $\boldsymbol{\Xi}$ to include the constraints, where the real or imaginary part of the constellation points is unable to exploit IE. Define a set $\boldsymbol{\Delta}$ to include the constraints where the real or imaginary part of the constellation points can be scaled for IE purpose. Hence, we obtain that

$$\text{card}\{\boldsymbol{\Xi}\} + \text{card}\{\boldsymbol{\Delta}\} = 2K_2, \tag{11}$$

where $\text{card}(\cdot)$ denotes the cardinality of a set. Substituting (3)$\sim$(7) into P1 yields a re-formulated problem

$$\begin{aligned} P2\ :&\underset{\boldsymbol{W}}{\text{argmin}}\ \textstyle\sum_{\iota=1}^{n}||\boldsymbol{W}\boldsymbol{s}^{(\iota)}||^2, \\ \text{s.t.}\ &(C5): |\Im\{\boldsymbol{h}_i\boldsymbol{W}\boldsymbol{s}^{(\iota)}(s_i^{(\iota)})^*\}| \leq \\ &\qquad (\Re\{\boldsymbol{h}_i\boldsymbol{W}\boldsymbol{s}^{(\iota)}(s_i^{(\iota)})^*\} - \sigma\sqrt{\bar{\Gamma}_i})\tan\theta, \forall i \in \mathbb{K}_1, \forall \iota \in n, \\ &(C6): \Re\{\boldsymbol{h}_j\boldsymbol{W}\boldsymbol{s}^{(\iota)}\} = \sigma\sqrt{\bar{\Gamma}_j}\Re\{s_j^{(\iota)}\}, \\ &\qquad \text{and}\ \Im\{\boldsymbol{h}_j\boldsymbol{W}\boldsymbol{s}^{(\iota)}\} = \sigma\sqrt{\bar{\Gamma}_j}\Im\{s_j^{(\iota)}\}, \forall j \in \mathbb{K}_2^{\boldsymbol{\Xi}}, \forall \iota \in n, \\ &(C7): \Re\{\boldsymbol{h}_j\boldsymbol{W}\boldsymbol{s}^{(\iota)}\} \geq (\text{or}\ \leq)\sigma\sqrt{\bar{\Gamma}_j}\Re\{s_j^{(\iota)}\}, \\ &\text{and}\ \Im\{\boldsymbol{h}_j\boldsymbol{W}\boldsymbol{s}^{(\iota)}\} \geq (\text{or}\ \leq)\sigma\sqrt{\bar{\Gamma}_j}\Im\{s_j^{(\iota)}\}, \forall j \in \mathbb{K}_2^{\boldsymbol{\Delta}}, \forall \iota \in n, \end{aligned} \tag{12}$$

where $\boldsymbol{h}_{i(\text{or } j)} = \boldsymbol{c}_{i(\text{or } j)}\boldsymbol{H}_{i(\text{or } j)} \in \mathbb{C}^{N_t \times 1}$ serves as the MISO channel with the effect of a local combiner. Now, the standard convex optimization P2 can be readily solved by CVX. The constraints (C5)$\sim$(C7) guarantee the subscribed SINR requirements for each sub-block. Compared to the classic SL MIE design, P2 indicates that the precoding matrix $\boldsymbol{W}$ is optimized across n symbol slots. Hence, though P2 is subject to more constraints than that of SL design, the precoder is only designed once for each sub-block. For completeness, we further provide some discussions on the near-optimality of the BL-MIE design, summarized in the followings Remarks.

Remark 1: Conventional IM designs require that each user's signal is transmitted along to the null space of other users' channels, which limits degrees-of-freedom (DoF) of the precoder. Differently, by the proposed BL-MIE design, it is not necessary to send each user's signal along the orthogonal space of others' channels. Accordingly, the superiority of the proposed design comes from concentrating the signal-of-interest along the channel that the users have high channel

gain, as well as guaranteeing the beneficial effect of MUI regardless of the modulation schemes. □

Remark 2: By accordingly setting the SINR requirements based on the users' modulation schemes, i.e., setting a low/moderate SINR for the low-order modulation users but a high SINR for the high-order modulation users, the proposed precoder is able to readily satisfy the users' distinct throughput requirements with a significant power reduction. In comparison, the classical IE precoder is designed for uniform modulation. As a result, it has to employ high-order modulation when part of users requires high throughput, even if others have relatively low throughput requirement, incurring unnecessary high power consumption. □

V. Computational Complexity Analysis of the BL-MIE Design

In this section, we present the analytic computational complexity analysis to obtain an explicit comparison between the BL-MIE and classic SL designs.

Lemma 1: With an interior-point based solver, the complexity of solving a conic optimization problem includes iteration complexity and per-iteration complexity. Assume that a generic optimization problem is subject to P linear constraints (including generic linear matrix inequalities) with size k_p of each constraint, as well as L second order cone constraints with size k_l of each constraint. 1) The iteration complexity is calculated as

$$C_{\text{ite}} = \ln(1/\epsilon)(\sum\nolimits_{p=1}^{P} k_p + 2L)^{1/2}, \tag{13}$$

where the term $\ln(1/\epsilon)$ relates to the accuracy setup for the ϵ-optimum, and the square root term specifies a barrier parameter corresponding to the geometric complexity of the constraints. 2) The per-iteration complexity is calculated as

$$C_{\text{per}} = \underbrace{o\sum\nolimits_{p=1}^{P} k_p^3 + o^2\sum\nolimits_{p=1}^{P} k_p^2 + o\sum\nolimits_{l=1}^{L} k_l^2}_{a} + \underbrace{o^3}_{b}, \tag{14}$$

where the terms in "a" and "b" correspond to the complexities on the generation and factorization of the variables in P2, respectively. Finally, the overall complexity is given as $C = C_{\text{ite}}C_{\text{per}}$ [13]. □

When designing mixed-modulation IE precoder at SL, the corresponding optimization problem can be revised based on P2, where the condition $\forall \iota \in n$ in the constraints can be removed. Hence, for a SL mixed-modulation precoder, its optimization problem is subject to $2K_1$ linear constraints of size 1, and $2K_2$ linear constraints of size 1. Based on Lemma 1, the per symbol slot complexity of the SL-MIE precoder is given by

$$\begin{aligned} C_{\text{SL-MIE}} = \ln(1/\epsilon)&\sqrt{2K_1 + 2K_2} \\ &\big(o(2K_1 + 2K_2) + o^2(2K_1 + 2K_2) + o^3\big), \end{aligned} \tag{15}$$

where o is on the order of $o = \mathcal{O}(N_tK)$. On the other hand, solving the sub-blocl level optimization P2 is subject to $2nK_1$ linear constrains in (C5) with size 1, and $2nK_2$ linear constants in (C6)$\sim$(C7) with size 1. Hence, the complexity of the P2 is given by

$$\begin{aligned} C_{\text{P2}} = \ln(1/\epsilon)&\sqrt{2nK_1 + 2nK_2}\cdot \\ &\big(o(2nK_1 + 2nK_2) + o^2(2nK_1 + 2nK_2) + o^3\big). \end{aligned} \tag{16}$$

Evidently, since P2 is designed for n consecutive symbol slots, the average per symbol slot complexity of the BL-MIE precoder is caculated as

$$C_{\text{BL-MIE}} = \frac{C_{\text{P2}}}{n} \approx \frac{C_{\text{SL-MIE}}}{\sqrt{n}}. \tag{17}$$

Remark 3: Compared to the classic SL precoder, the BL-MIE precoder reduces the complexity, roughly on the order of $\sqrt{n}$. Hence, the BL-MIE design well strikes the tradeoff between the complexity and system performance. In particular, the BL-MIE reduces to classic SL design with $n = 1$. □

Remark 4: It is worth noting that, when n is comparable to N_tK, the per-iteration complexity in (16) is dominated by the generation of the optimization variables, where the gain of the complexity reduction by the BL-MIE degrades. A extreme case would be $n \to \infty$, where the factorization complexity is fully negligible. As a result, the complexity of the BL-MIE design would be higher than that of the SL precoder on the order of $\sqrt{n}$. Hence, it is preferable to set a proper value of n, typically $n < N_tK$, for achieving a low complexity. This will be further discussed in simulation part. □

VI. Simulation Results

We present the Monte-Carlo simulation results in this section. It is assumed that the BS is equipped with $N_t = 10$ antennas to serve $K = 10$ users, where each user is equipped with $N_r = 5$ receive antennas. Without loss of generality, assume that there are $K_1 = 5$ users having low throughput requirement supported by QPSK modulation, and $K_2 = 5$ users requiring high throughput supported by 16-QAM. The transmitted vector $\boldsymbol{s}^{(\iota)}$ at each symbol-slot is randomly generated. Rayleigh fading channel is adopted, and the power budget $p_{\max}$ is set to as 60 dBm. Noise variance is set to as $\sigma^2 = 0.01$ except in Fig. 2(a). The following precoders are selected as benchmarks. 1) The classical IE precoder with uniform QPSK [1] or 16-QAM modulation [10]. 2) The ZF precoder [14], which treats the input alphabet as infinite Gaussian signal and its structure is not related to the transmitted symbols. For fair comparison, the combiner of the benchmarks is calculated by the largest singular vector of the MIMO channel.

In Fig. 2(a), we show the power consumption performance at different noise levels. It is observed that the BL-MIE design achieves 4 dB power saving over the ZF precoder, and is more power-efficient than the IE precoder with 16-QAM. Although the ML-MIE consumes more power than the classic IE precoder with QPSK, the latter only achieves low throughput and can not satisfy the heterogeneous requirements, which will be further analyzed in Fig. 2(b). It is because the rich MUI can be utilized as a beneficial component, rather than being strictly mitigated by the ZF precoder. Also, the BL-MIE precoder is able to serve the users having heterogeneous throughput requirements with distinct modulation schemes, while the classical IE precoder has to employ uniform high-order modulation even though part of the users has relatively low throughput requirement, incurring high power consumption. Also, since the BL-MIE precoder needs to guarantee the subscribed SINR across n symbol slots, the incurred power is higher than that of the classic SL-MIE precoder.

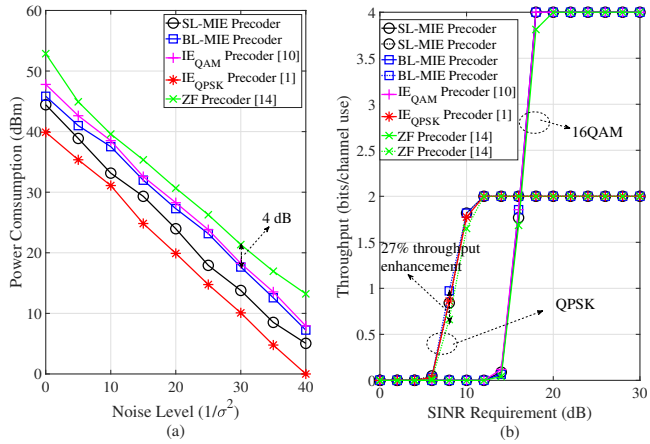

Fig. 2. The impact of the noise level on the power consumption and throughput performance, where the SINR requirements are set to as 7 dB for QPSK users and 10 dB for 16-QAM users.

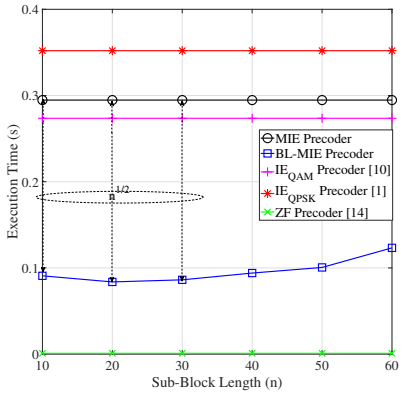

Fig. 3. The impact of the sub-block length on the execution time.

In Fig. 2(b), we demonstrate the throughput performance under different SINR requirements. It can be seen that, the BL-MIE precoder is able to adopt mixed modulation to satisfy the users' distinct throughput requirements. Since the BL-MIE precoder is able to make the MUI always constructive regardless of the modulation schemes, both the QPSK and 16-QPSK users can achieve 5%-27% throughput enhancement over the ZF precoder. As comparisons, by the classical IE precoder with 16-QAM modulation, the users having low throughput requirement are still served by 16-QAM, which needs at least 16 dB for achieving a comparable throughput that is achieved at 12 dB of QPSK modulation, resulting in an increased power consumption as demonstrated in Fig. 2(a). By the IE precoder with QPSK modulation, its throughput is saturated at 2 bits/channel use and thus cannot satisfy any throughput higher than this threshold. Also, while optimizing precoder at a sub-block level, the BL-MIE still guarantees the SINR requirement for all the symbol slots, thus providing close throughput to the classic SL precoder.

In Fig. 3, the average per symbol slot execution time is demonstrated. It can be seen that the BL-MIE significantly reduces the computational complexity approximately on the order of $\mathcal{O}(\sqrt{n})$, as proved by Remark 3. Also, it is observed that the complexity reduction gain decreases with the increase of n. It is because with a larger value of n, the term o^3 in (16) becomes a negligible component. Hence, it is preferable to set a moderate value for n, i.e., $n < N_t K$.

VII. Conclusion

Focusing on the MU MIMO transmission, we have proposed a unified IE framework for sub-block level mixed-modulation scenario. A power minimization oriented BL-MIE precoder is proposed. It only needs to be optimized across n consecutive symbols slots, and MUI is made always constructive for the users having distinct modulation schemes. It has been proved that the BL-MIE approximately reduces the computational complexity on the order of $\mathcal{O}(\sqrt{n})$, and thus well strikes the tradeoff between the transmit-power consumption and computational complexity. Simulation results have confirmed that the proposed design achieves up to 4 dB power saving over the classical IE and ZF precoders, and simultaneously is able to obtain up to 5%-27% throughput enhancement over the benchmarks.

References

[1] C. Masouros and G. Zheng, "Exploiting known interference as green signal power for downlink beamforming optimization" *IEEE Trans. Sig. Proc.*, vol. 63, no. 14, pp. 3668-3680, Jul 2015.

[2] F. Sohrabi and W. Yu, "Hybrid digital and analog beamforming design for large-scale antenna arrays," *IEEE J. Sel. Topics Sig. Proc.*, vol. 10, no. 3, pp. 501-513, Apr. 2016.

[3] C. Masouros and E. Alsusa, "A novel transmitter-based selective precoding technique for DS/CDMA systems," *IEEE Signal Process. Lett.*, vol. 14, no. 9, pp. 637–640, Sep. 2007.

[4] D. Spano, M. Alodeh, S. Chatzinotas, and B. Ottersten, "Symbol level precoding for the non-linear multiuser MISO downlink channel," *IEEE Trans. Signal Process.*, vol. 66, no. 5, pp. 1331-1345, Mar. 2018.

[5] S. Domouchtsidis, C. G. Tsinos, S. Chatzinotas, and B. Ottersten, "Symbol-level precoding for low complexity transmitter architectures in large-scale antenna array systems," *IEEE Trans. Wireless Commun.*, vol. 18, no. 2, pp. 852-863, Feb. 2019.

[6] G. Hegde, C. Masouros, M. Pesavento, "Coordinated Hybrid Precoding for Interference Exploitation in Heterogeneous Networks", *IEEE Commun. Lett.*, vol. 23, no. 11, Nov. 2019.

[7] Z. Wei, C. Masouros, K. Wong, and X. Kang, "Multi-cell interference exploitation: A new dimension in cell coordination", *IEEE Trans. Wireless Commun.*, vol. 19, no. 1, pp. 1303-1312, Oct. 2019.

[8] Z. Wei, F. Liu and C. Masouros, "Secure directional modulation with few-bit phase shifters: Optimal and iterative-closed-form designs", *IEEE Trans. Commun.*, vol. 69, no. 1, pp. 486-500, Oct. 2020.

[9] Q. Xu, P. Ren, A. L. Swindlehurst, "Rethinking secure precoding via interference exploitation: A smart eavesdropper perspective," *IEEE Trans. Inf. Forensics Secur.*, vol. 16, pp. 585-600, Aug. 2020.

[10] A. Li, C, Masouros, B. Vucetic, A. Swindlehurst, "Interference exploitation precoding for multi-level modulations: Closed-form solutions," *IEEE Trans. Wireless Commun.*, vol. 61, no. 1, pp. 291-308, Jan. 2021.

[11] T. Xu, F. Liu, A. Li, C. Masouros, and I. Darwazeh, "Constructive interference precoding for reliable non-orthogonal IoT signaling," in *Proc. IEEE INFOCOM*' 19, Paris, France.

[12] A. Li, C. Masouros, and A. Swindlehurst, "Practical interference exploitation precoding without symbol-by-symbol optimization: A block-level approach," *IEEE Trans. on Wireless Commun.*, vol. 22, no. 6, pp. 3982-3996, Jun. 2023.

[13] K. Wang *et al.*, "Outage constrained robust transmit optimization for multiuser MISO downlinks: Tractable approximations by conic optimization," *IEEE Trans. on Signal Process.*, vol. 62, no. 21, pp. 5690-5705, Dec. 2014.

[14] A. Wiesel, Y. C. Eldar, and S. Shamai, "Zero-forcing precoding and generalized inverses, " *IEEE Trans. Signal Process.*, vol. 56, no. 9, pp. 4409-4418, Sep. 2008.